3-31-2007

Deviations from ozone photostationary state during the International Consortium for Atmospheric Research on Transport and Transformation 2004 campaign: Use of measurements and photochemical modeling to assess potential causes

Robert J. Griffin
University of New Hampshire, Durham

Pieter J. Beckman
University of New Hampshire, Durham

Robert W. Talbot
University of New Hampshire, Durham

Barkley C. Sive
University of New Hampshire, Durham

Ruth K. Varner
University of New Hampshire, Durham, ruth.varner@unh.edu

Recommended Citation
Griffin R. J., P. J. Beckman, R. W. Talbot, B. C. Sive, R.K. Varner (2007), Deviations from ozone photostationary state during the International Consortium for Atmospheric Research on Transport and Transformation 2004 campaign: Use of measurements and photochemical modeling to assess potential causes, J. Geophys. Res., 112, D10S07, doi:10.1029/2006JD007604.

Deviations from ozone photostationary state during the International Consortium for Atmospheric Research on Transport and Transformation 2004 campaign: Use of measurements and photochemical modeling to assess potential causes

Robert J. Griffin,[1,2] Pieter J. Beckman,[1] Robert W. Talbot,[1] Barkley C. Sive,[1] and Ruth K. Varner[1]

Received 31 May 2006; revised 25 October 2006; accepted 28 December 2006; published 31 March 2007.

[1] Nitric oxide (NO) and nitrogen dioxide (NO_2) were monitored at the University of New Hampshire Atmospheric Observing Station at Thompson Farm (TF) during the ICARTT campaign of summer 2004. Simultaneous measurement of ozone (O_3), temperature, and the photolysis rate of NO_2 (j_{NO2}) allow for assessment of the O_3 photostationary state (Leighton ratio, Φ). Leighton ratios that are significantly greater than unity indicate that peroxy radicals (PO_2), halogen monoxides, nitrate radicals, or some unidentified species convert NO to NO_2 in excess of the reaction between NO and O_3. Deviations from photostationary state occurred regularly at TF ($1.0 \leq \Phi \leq 5.9$), particularly during times of low NO_x ($NO_x = NO + NO_2$). Such deviations were not controlled by dynamics, as indicated by regressions between Φ and several meteorological parameters. Correlation with j_{NO2} was moderate, indicating that sunlight probably controls nonlinear processes that affect Φ values. Formation of PO_2 likely is dominated by oxidation of biogenic hydrocarbons, particularly isoprene, the emission of which is driven by photosynthetically active radiation. Halogen atoms are believed to form via photolysis of halogenated methane compounds. Nitrate radicals are believed to be insignificant. Higher Φ values are associated with lower mixing ratios of isoprene and chloroiodomethane and lower ratios of NO_x to total active nitrogen, indicating that photochemical aging may very well lead to increased Φ values. PO_2 levels calculated using a zero-dimensional model constrained by measurements from TF can account for 71% of the observed deviations on average. The remainder is assumed to be associated with halogen atoms, most likely iodine, with necessary mixing ratios up to 0.6 or 1.2 pptv, for chlorine and iodine, respectively.

Citation: Griffin, R. J., P. J. Beckman, R. W. Talbot, B. C. Sive, and R. K. Varner (2007), Deviations from ozone photostationary state during the International Consortium for Atmospheric Research on Transport and Transformation 2004 campaign: Use of measurements and photochemical modeling to assess potential causes, *J. Geophys. Res.*, *112*, D10S07, doi:10.1029/2006JD007604.

1. Introduction

[2] The oxides of nitrogen (NO_x) consist of nitric oxide (NO) and nitrogen dioxide (NO_2). NO_x species are emitted from high-temperature combustion processes as a result of the combination of oxygen and nitrogen atoms/molecules [*Glassman*, 1996]. NO also has biogenic soil and plant sources that result in its release to the atmosphere [*Ludwig et al.*, 2001; *Hari et al.*, 2003].

[3] NO_x species play a crucial role in the formation of tropospheric ozone (O_3). While stratospheric O_3 protects the Earth and its inhabitants from harmful ultraviolet (UV) radiation [*Finlayson-Pitts and Pitts*, 2000], O_3 in the troposphere is also a photochemical pollutant that causes damage to surfaces, oxidizes lung tissue, and affects secondary chemistry in the atmosphere, as discussed in the review by *Seinfeld* [2004]. For example, the reaction between O_3 and monoterpenes is a major source of secondary organic aerosol (SOA) in the atmosphere [*Hoffmann et al.*, 1997; *Griffin et al.*, 1999; *Gao et al.*, 2004].

[4] In the troposphere, a molecule of NO_2 is degraded photochemically to form a molecule of NO and an oxygen atom (O). It should be noted that this process depends on the sufficient flux of photons associated with light of the appropriate wavelength to photolyze NO_2. The O atom quickly reacts with molecular oxygen (O_2) in the presence of a third body to form O_3. However, the O_3 formed can

[1]Climate Change Research Center, Institute for the Study of Earth, Oceans, and Space, University of New Hampshire, Durham, New Hampshire, USA.
[2]Also at Department of Earth Sciences, University of New Hampshire, Durham, New Hampshire, USA.

0148-0227/07/2006JD007604

react rapidly with the NO to reform NO_2 and O_2. The net result of these reactions is a null cycle, and when steady state is assumed, the O_3 concentration can be predicted as [*Seinfeld and Pandis*, 1998]

$$[O_3] = \frac{j_{NO2}[NO_2]}{k_1[NO]} \quad (1)$$

where the bracket notation represents a concentration or mixing ratio (here, parts per billion by volume, ppbv), j_{NO2} (s^{-1}) is the photolysis rate of NO_2, and k_1 ($ppbv^{-1}\,s^{-1}$) is the temperature-dependent rate constant for the reaction between NO and O_3. This is referred to as the photostationary state for O_3. If each side of equation (1) is divided by $[O_3]$, the right hand side is termed the Leighton ratio, Φ [*Leighton*, 1961]:

$$\Phi = \frac{j_{NO2}[NO_2]}{k_1[NO][O_3]} \quad (2)$$

[5] Numerous studies have investigated adherence to/deviation from Leighton ratios approximately equal to unity. In general, it has been shown that in areas with high NO_x levels, Leighton ratios are consistently equal to unity [*Stedman and Jackson*, 1975; *Calvert and Stockwell*, 1983; *Shetter et al.*, 1983; *Parrish et al.*, 1986; *Carpenter et al.*, 1998; *Thornton et al.*, 2002; *Yang et al.*, 2004]. Other locations generally show that Φ values ranging from 1.2 to approximately 3.0 are applicable for high-sun conditions in more rural or isolated locations [*Ridley et al.*, 1992; *Cantrell et al.*, 1993; *Hauglustaine et al.*, 1996; *Rohrer et al.*, 1998; *Volz-Thomas et al.*, 2003]. Measurements made at increased elevation have led to calculations that result in generally higher averages and ranges for Φ [*Davis et al.*, 1993; *Crawford et al.*, 1996; *Mannschreck et al.*, 2004].

[6] The value of Φ deviates positively from unity when some chemical process other than the reaction between NO and O_3 converts NO to NO_2. One major pathway for this is the reaction between NO and a peroxy radical (PO_2), either organic (RO_2) or hydro (HO_2) ($PO_2 = RO_2 + HO_2$). RO_2 and HO_2 generally result from the atmospheric oxidation of volatile organic compounds (VOCs) and/or carbon monoxide (CO). Such reactions lead to the formation of photochemical O_3 as a tropospheric pollutant [*Seinfeld and Pandis*, 1998]. An additional pathway by which NO can be converted to NO_2 without concomitant consumption of O_3 is via halogen monoxide (XO, where X represents a halogen atom) reactions. For example, molecular chlorine (Cl_2) can be released from sea salt particles [*Knipping et al.*, 2000] or directly emitted from swimming pools and cooling towers [*Chang et al.*, 2002]. Cl_2 is photolabile and forms chlorine atoms (Cl) upon degradation. Photolabile halogenated methane compounds such as chloroiodomethane (CH_2ClI) may also release iodine (I) upon photolysis [*Rattigan et al.*, 1997; R. K. Varner et al., Observations of chloroiodomethane from coastal North Atlantic and remote Pacific regions, manuscript in preparation, 2007, hereinafter referred to as Varner et al., manuscript in preparation, 2007]. The resulting X may form the corresponding XO, which reacts with NO, converting NO to NO_2 and reforming X. Nitrate radical (NO_3) also reacts with NO to form two molecules of NO_2. However, because of its rapid photolysis, NO_3 is considered negligible for this study. Negative deviations of calculated Φ from unity may occur when rapid changes in the NO mixing ratio or j_{NO2} occur, such that the system may not have achieved steady state. Positive and negative deviations from unity of calculated Φ values may also be associated with instrumental uncertainties.

2. Measurements

[7] The International Consortium for Atmospheric Research on Transport and Transformation (ICARTT) (July–August 2004) was a multinational, multiagency large measurement, modeling, and forecast campaign aimed at characterizing the atmospheric processes that control the spatial and temporal profiles of air pollutants such as O_3 and aerosols in New England [*Fehsenfeld et al.*, 2006]. An additional aim of ICARTT was a semi-Lagrangian study of air pollution to investigate pollution inflow to, transformation in, and outflow from New England. ICARTT included ground measurements, ship-based measurements, airborne (airplane-, balloon-, and satellite-based) measurements, air quality forecasting, and modeling analyses. More detailed information regarding each of these platforms is available on the Web site of the National Oceanic and Atmospheric Administration (NOAA) (http://www.al.noaa.gov/ICARTT/).

[8] The University of New Hampshire (UNH)/NOAA AIRMAP Cooperative Institute has established a network of five atmospheric observing stations in New Hampshire and Maine. The AIRMAP stations measure the concentrations of approximately 180 species, as well as additional meteorological parameters relevant to atmospheric chemistry and climate, on a continuous year-round basis with a time resolution varying from 1 min to 24 hours. In this study, 1-min-average records for all relevant data are used (except where noted) from the UNH Atmospheric Observatory at Thompson Farm (henceforth called TF). Ozone mixing ratios are measured using UV spectroscopy, CO is measured using infrared spectroscopy, mixing ratios of total active nitrogen (NO_y) are made using a chemiluminescent technique, and j_{NO2} is measured using filter radiometry. For reference, j_{NO2} approaches a value of 0.01 s^{-1} at TF at noon on a clear summer day. A discussion of filter radiometric techniques is given by *Lefer et al.* [2001]; manufacturer specifications indicate an uncertainty of approximately 3% on the measured photolysis rates. However, *Lefer et al.* [2001] indicate largest uncertainties under conditions of high solar zenith angle. VOC data are collected hourly over 10-min sampling periods and analyzed by gas chromatography as described by *Griffin et al.* [2004a], *Sive et al.* [2005], *Talbot et al.* [2005], *Zhou et al.* [2005], and Y. Zhou et al. (Bromoform and dibromomethane measurements in the seacoast region of New Hampshire, 2002–2004, submitted to *Journal of Geophysical Research,* 2006, hereinafter referred to as Zhou et al., submitted manuscript, 2006). Information on measurement techniques for additional species can be found on the AIRMAP website (http://www.airmap.unh.edu). TF is located in Durham, NH (43.11°N,

70.95°W), slightly above sea level (24 m); Durham, NH, is located approximately 15 km inland from the Atlantic Ocean and approximately 90 km north of Boston, MA. More complete descriptions of the AIRMAP/UNH atmospheric observing stations and additional information on data collection and availability are provided by *DeBell et al.* [2004], *Mao and Talbot* [2004], and *Talbot et al.* [2005].

[9] Particular attention is paid here to the measurement of NO_x. In July 2004, a fast-response, high-sensitivity instrument for measurement of NO and NO_2 was installed at TF. At TF, samples are drawn into a manifold that has an inlet located atop a 40-foot instrumented, walk-up sampling tower. The NO_x instrument pulls a subsample from this manifold. The sample within the NO_x instrument is passed through a narrow-band photolysis cell. When the shutter on this cell is closed, NO_2 is not photolyzed; conversely, when it is open, NO_2 is converted to NO with some efficiency. After passing through the photolysis cell, the sample is passed into a reaction chamber in which excess O_3 has been generated. The reaction between NO and O_3 is chemiluminescent, meaning that photons are given off during its procession. These photons are measured, and the signal is converted to a mixing ratio of NO. When the shutter is closed, the system measures only NO. When the shutter is open, the system is measuring ambient NO plus the ambient NO_2 that has been converted to NO. The difference between these two measurements is attributed to NO_2 that has been converted to NO. The shutter alternates between open and closed with a frequency of 3 min. Instrument zeros are performed every 20 to 30 min, and calibrations for NO are performed as standard additions approximately every four hours. Calibration of the efficiency of conversion of NO_2 to NO in the photolysis cell was performed approximately once per week. The lower detection limits (LDLs) for this instrument are approximately 5 pptv and 13 pptv for NO and NO_2, respectively, with corresponding uncertainties of 5% and 10%. More detailed information on the instrument and its predecessors is given by *Ryerson et al.* [2000].

[10] Uncertainty in the calculation of the Φ values presented here was considered by investigating those points in time when j_{NO2} was between 0.001 and 0.002 s^{-1}, during which very little influence of PO_2 and X should be observed because each of these species is derived photochemically. Therefore Φ should be unity during these times [*Thornton et al.*, 2002]. For the entire sampling period, the average Φ value calculated using equation (2) during these times was 1.04 ± 0.2 (one standard deviation, SD). Therefore Φ values between 0.84 and 1.24 cannot be considered to be out of photostationary state for this study. This uncertainty range is on par with those used in previous work [*Cantrell et al.*, 1993; *Crawford et al.*, 1996; *Carpenter et al.*, 1998] but is smaller than that which results from a standard propagation of errors technique (approximately ±0.35).

[11] Data from the 3-week period from 26 July through 15 August 2004 are considered here. The official start of the ICARTT campaign was 1 July 2004. However, during the early and middle part of July, the shutter that controlled the measurement of NO_2 was not operating properly. This shutter was fixed on 19 July 2004. However, TF suffered a power outage on 21 July 2004. It took several days to repair the cause of the outage and reestablish proper operation of the NO_x instrument. Therefore only data from 26 July through 15 August 2004 are considered.

3. Results and Discussion

3.1. Campaign-Long Results

[12] It is of interest first to characterize the New Hampshire atmosphere during July and August of 2004 with respect to NO_x constituents, NO_y, CO, and O_3. CO and O_3 indicate the relative importance of primary emissions and secondary processing, respectively [*Fishman and Seiler*, 1983]. Figure 1 shows the 1-min average mixing ratios of NO and NO_2 at TF for 26 July through 15 August 2004. During this time period, it can be seen that NO_2 was generally higher than NO, except for occasional spikes of NO that generally occurred late morning local time, indicating that photolysis of NO_2 at this time was occurring more rapidly than O_3 was being titrated by NO. The range of NO measured was from 0.005 ppbv (= 5 pptv, the LDL of the instrument) to 6.45 ppbv, with a total of 17,642 measured points. The average NO mixing ratio was 0.26 ± 0.52 (SD) ppbv. Note that these values are calculated without consideration of those times when the NO mixing ratio was below the LDL of the instrument (total of 28 1-min points), meaning that the average values presented here are inflated very slightly. A Thermo Environmental Instruments (TEI, Woburn, MA) Model 42C-TL chemiluminescent NO_x monitor operated without a converter so as to measure only NO was also operated at TF over the course of the ICARTT campaign. This instrument also provides 1-min average data. Details of its operation are discussed by *Griffin et al.* [2004a] and are available on the AIRMAP website. To confirm the operation of the new NO/NO_2 instrument, the NO measurements from each instrument are compared. A linear regression between the NO mixing ratios of the TEI instrument (y variable) and those from the new combined NO/NO_2 instrument (x variable) results in a slope of 0.96, an intercept of 0.01, and an R^2 of 0.95 (not shown). Only times when both instruments measured NO above their individual LDLs are considered for this regression.

[13] Because of the lack of a photolytic loss process, NO_2 mixing ratios were highest at night. Conversion of NO_2 to nitric acid (HNO_3) through reaction with the hydroxyl radical (OH) is also expected to lead to loss of NO_2 during the day [*Seinfeld and Pandis*, 1998]. At night, NO_2 conversion to dinitrogen pentoxide (N_2O_5) with subsequent conversion to HNO_3 is also a chemical loss process for NO_2 [*Seinfeld and Pandis*, 1998]. Over the course of the ICARTT campaign, the range of measured NO_2 mixing ratios was 0.02 to 12.05 ppbv for 9,653 data points, with only a very small number (3) of measurements found to be below the LDL. The average NO_2 mixing ratio at TF during this part of the ICARTT campaign was 2.07 ± 1.66 (SD) ppbv.

[14] The total NO_x and NO_y measured at TF during the same period are shown in Figure 2. NO_x makes up a significant fraction of NO_y under most scenarios, but times of definite deviation are observed (for example, 11 August 2004). Total NO_x mixing ratios for times when both NO and NO_2 are above the instrument LDLs range from 0.21 ppbv to 17.54 ppbv, with an average of 2.33 ± 1.93 (SD) ppbv. The

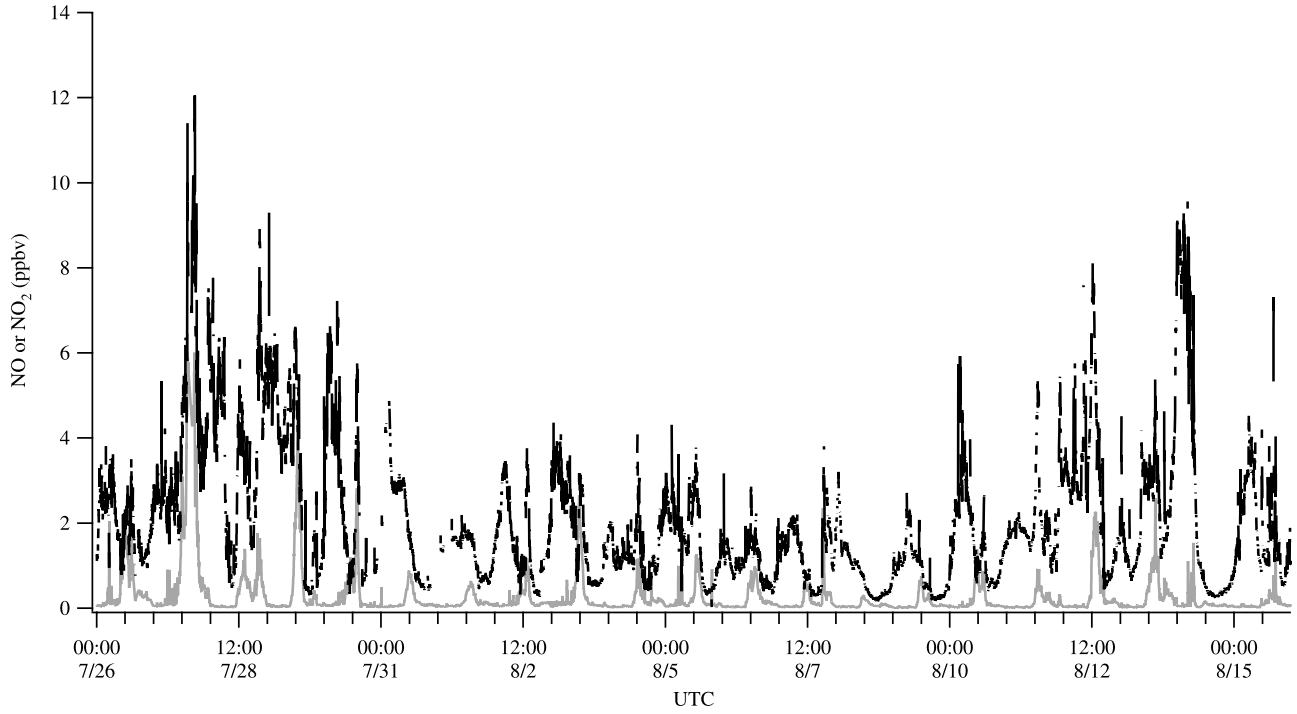

Figure 1. NO (shaded) and NO_2 (solid) mixing ratios (ppbv) at TF over the course of the ICARTT campaign.

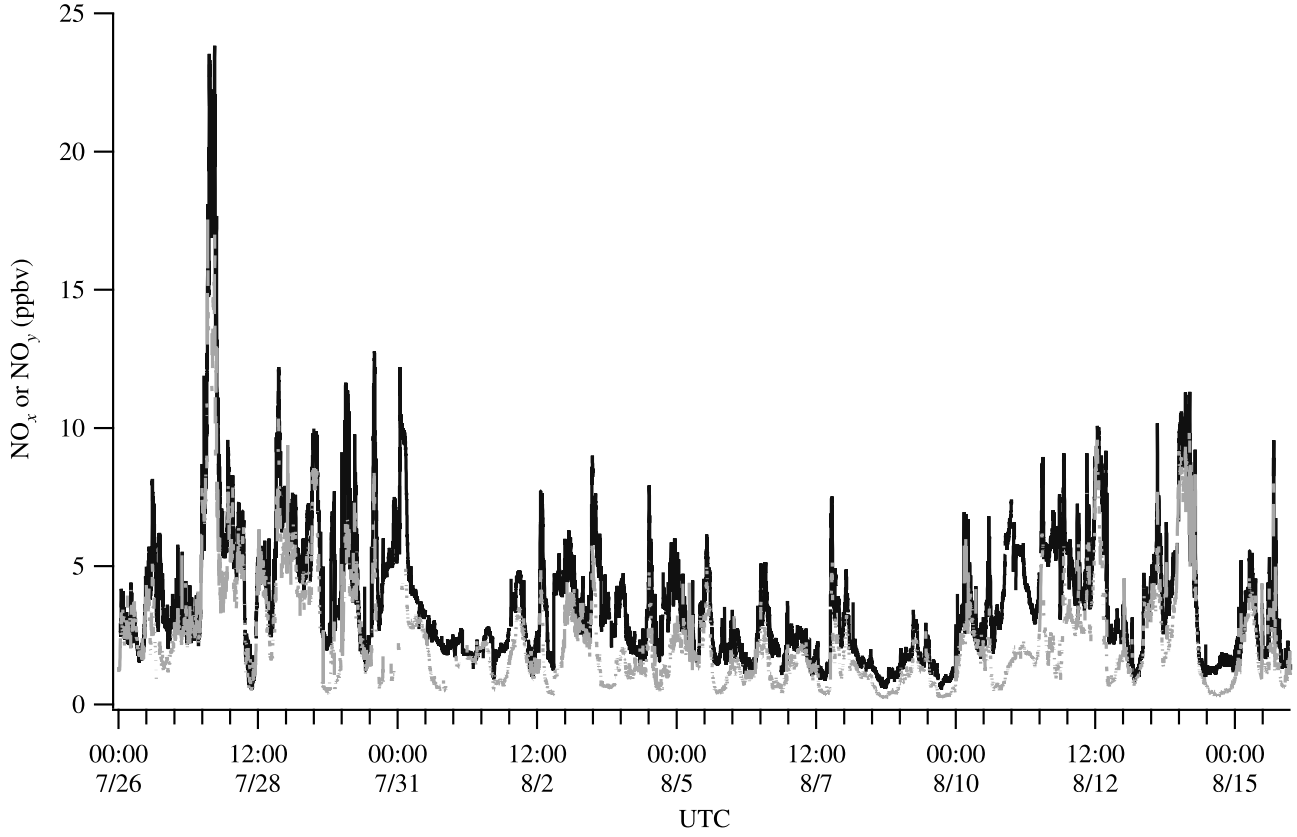

Figure 2. Total measured NO_x (shaded) and NO_y (solid) mixing ratios (ppbv) at TF over the course of the ICARTT campaign.

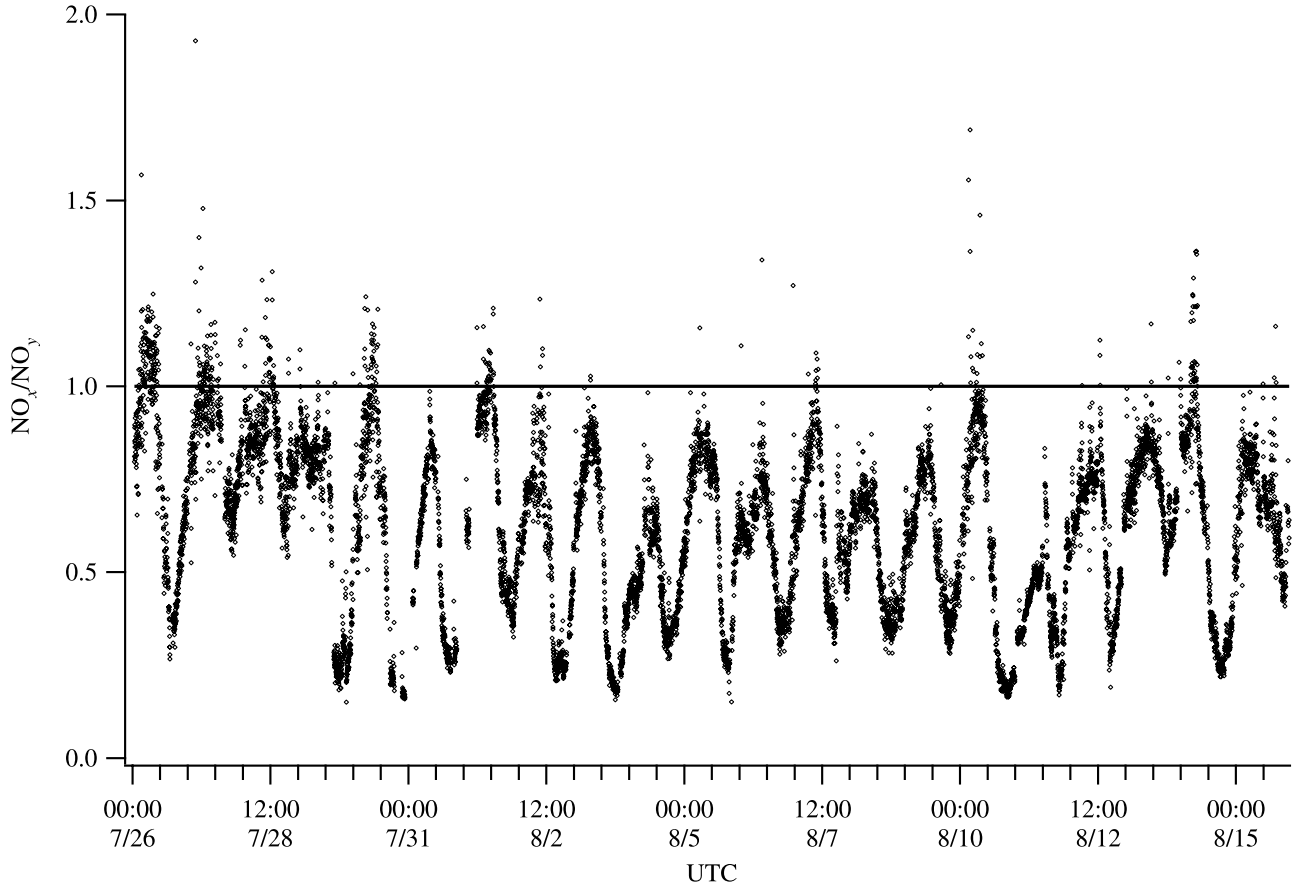

Figure 3. Ratio (dimensionless) of total measured NO_x to total measured NO_y at TF over the course of the ICARTT campaign.

corresponding NO_y values ranged from 0.52 to 23.83 ppbv, with an average value of 3.67 ± 2.51 (SD) ppbv. The high end of the range of measured NO_y values all occurred on 27 July 2004; this was the only date on which NO_y levels exceeded 20 ppbv. NO_y values greater than 20 ppbv have been associated with hydrocarbon-sensitive or NO_x-saturated O_3 chemistry [*Sillman*, 1995]. Similar levels of NO_y were observed at this same site during a similar time period during the New England Air Quality Study (NEAQS) of 2002 [*Griffin et al.*, 2004a].

[15] The ratio of NO_x to NO_y indicates photochemical processing of pollutants because it can generally be assumed that the majority of NO_y is emitted in the form of NO_x [*Nunnermacker et al.*, 1998]. In general, daytime values of this ratio below 0.3 indicate a highly processed air mass, while those above 0.3 are representative of fresher emissions [*Trainer et al.*, 1993; *Chin et al.*, 1994]. Values for this ratio approach unity at night. For those times when both NO_x and NO_y measurements are available, the ratio of NO_x to NO_y is shown in Figure 3, which also includes a solid line indicating a value of unity. In general, a diurnal pattern for this ratio is observed, with the minimum values (overall minimum value of 0.15 occurring at 2057 UTC on 29 July 2004, range of daily minimum values of 0.15 to 0.55) occurring during the afternoon (generally between 1600 to 0030 UTC). The value of this ratio approached unity daily during the 3-week sampling period, with this generally occurring overnight or early morning local time.

[16] Concentrations of HNO_3 (a major component of NO_y) in New England decrease overnight because of depositional losses and the lack of a photochemical source that outweigh its nighttime formation via hydrolysis of N_2O_5, as was observed during NEAQS [*Brown et al.*, 2004; *Dibb et al.*, 2004]. Other non-NO_x contributors to NO_y (including alkyl nitrates and peroxy acetyl nitrate) are also expected to decrease overnight as a result of the lack of a photochemical source. Therefore NO and NO_2 are expected to be the major contributors to NO_y overnight (leading to a ratio of unity) because NO is continually emitted from combustion sources regardless of time of day and because photolysis of NO_2 ceases after sundown. The majority of NO_x overnight is expected generally to be in the form of NO_2 because any emitted NO will react rapidly with any residual O_3 from the previous day. The lack of significant NO mixing ratios at night is confirmed by the measurements shown in Figure 1.

[17] The distributions of O_3 and CO at TF during the same time period are shown in Figure 4. CO is used as a tracer of both short- and long-range transport of primary combustion emissions [*Fishman and Seiler*, 1983], while O_3 is an indicator of photochemical activity, as discussed previously. In combination, these measurements give an overall picture of the atmosphere at TF.

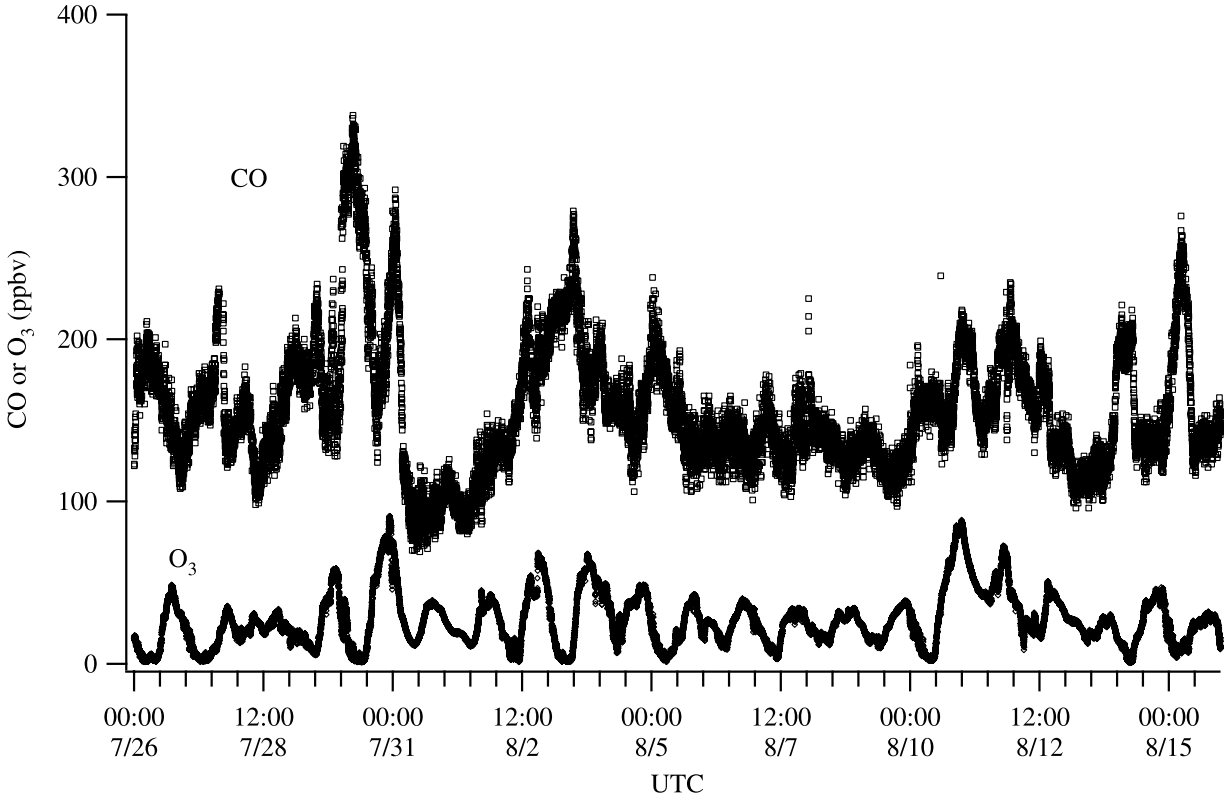

Figure 4. CO and O_3 mixing ratios (ppbv) at TF over the course of the ICARTT campaign.

[18] In general, CO varied between 100 and 200 ppbv diurnally, except for a pollution event that occurred 29 and 30 July 2004, when peak CO reached a value of 338 ppbv. This pollution event is also captured in the O_3 temporal profile, as peaks in O_3 reached upward of 90 ppbv during this time period; this value is significantly greater than the background mixing ratio of O_3 during summer in southeastern New Hampshire [*Mao and Talbot*, 2004]. The minimum CO mixing ratio (68 ppbv) was observed on 31 July 2004. The average CO mixing ratio during this time period was 157 ± 40 (SD) ppbv. Because of the much stronger diurnal variability of O_3, no range, average value, or standard deviation are given for this pollutant. However, it is interesting to note that a larger than average O_3 peak (88 ppbv) occurred late on 11 August 2004, the same day on which significant deviations between NO_x and NO_y occurred, as shown in Figures 2 and 3. Ozone peaks and deviation between NO_x and NO_y indicate photochemical processing.

[19] Figure 5 indicates the values of Φ calculated using equation (2) when the requisite mixing ratios of NO, NO_2, and O_3 are available from the measurements. Values for j_{NO2} are also required, as is the temperature in order to calculate k_1. In addition, certain data points have been removed from Figure 5. Times between 2000 and 0500 local time are not included. Only points in time with j_{NO2} values greater than or equal to 0.001 s^{-1} are considered. In addition, those points in time when j_{NO2} or the NO level changed rapidly were taken into account [*Parrish et al.*, 1986; *Carpenter et al.*, 1998]. A time interval, τ (min), required for NO to readjust to photostationary state at a level of 90% is defined, similar to *Yang et al.* [2004]:

$$\tau = \frac{1}{60}\left(\frac{-\ln(0.1)}{j_{NO2} + k_1[O_3]}\right) \quad (3)$$

When the change in j_{NO2} or NO mixing ratio between successive measurements was greater than 10%, calculated Φ values over the next τ minutes are removed from the analysis. For the remaining 3,561 data points, a regression of measured NO_2 mixing ratios versus those calculated assuming that Φ = 1 yields a slope of 0.94 and a R^2 of 0.97 when the intercept is forced to zero, as indicated in Figure 6. However, this type of regression is considerably misleading. Despite this strong correlation, 58% of the data points that are included in the regression fall outside of the $0.84 \leq \Phi \leq 1.24$ range indicated by the two additional solid lines in Figure 6.

[20] The values of Φ indicated in Figure 5 show the clear diurnal pattern of this parameter, with lowest values occurring at times of high solar zenith angle. Lowest values were less than unity, most likely because of uncertainty or error in the j_{NO2} values used; these values were generally within 10% of 0.84. In all, only 154 points (4% of all Φ data points) were associated with Φ values less than 0.84. The daily minimum values ranged from 0.5 (7 August 2004) to 1.07 (31 July 2004). Peak values generally occurred during times of peak photochemical activity. The daily peak values range from 1.41 (27 July 2004) to 5.87 (7 August 2004). Considering the entire 3-week data set and only those

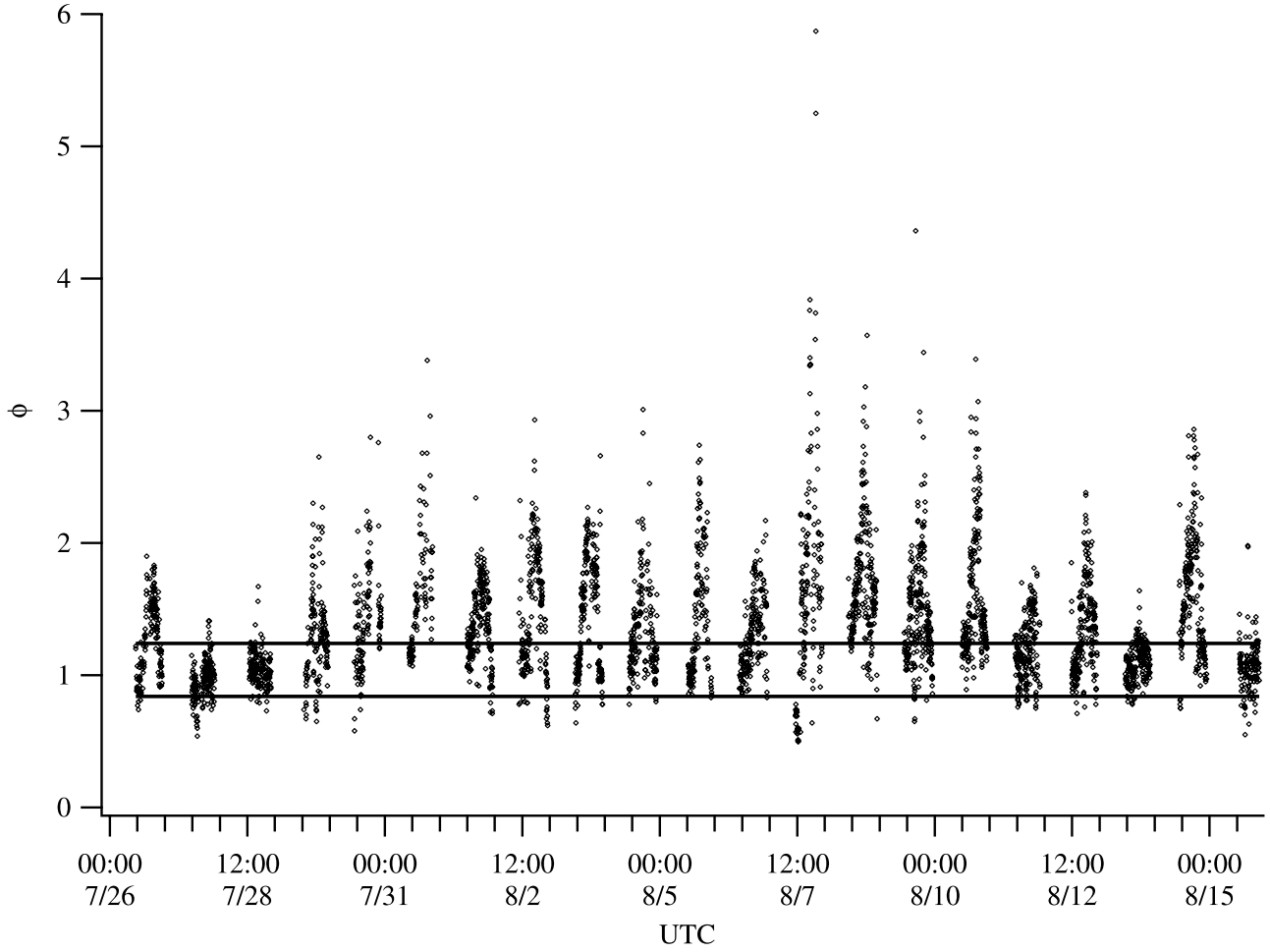

Figure 5. Values of the Leighton ratio at TF over the course of the ICARTT campaign. Solid lines indicate the range of Φ values that would be considered within photostationary state on the basis of measurement uncertainties.

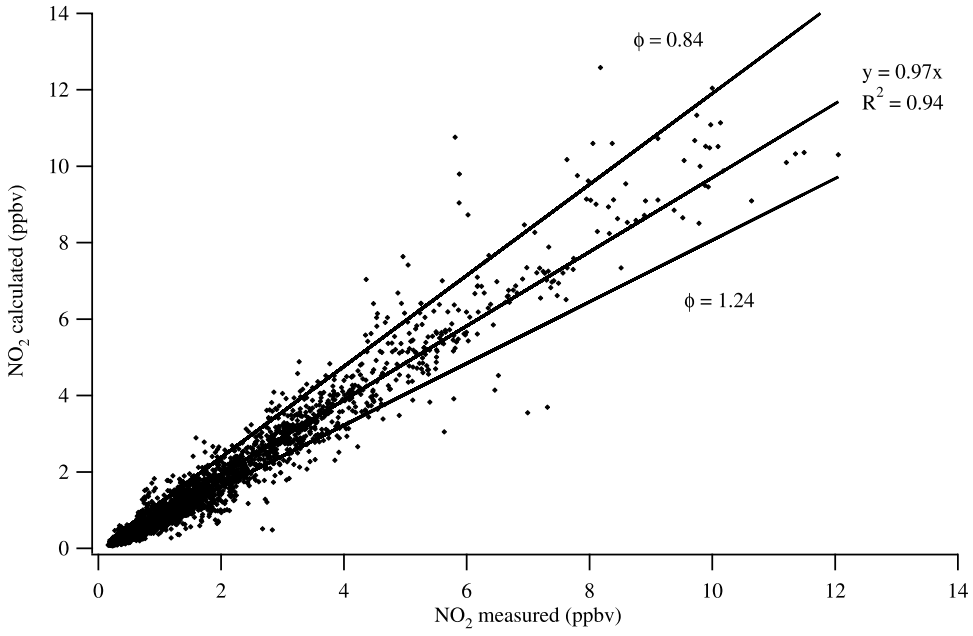

Figure 6. A regression between measured and predicted mixing ratios of NO_2. Predictions are based on an assumed Φ value of 1.0.

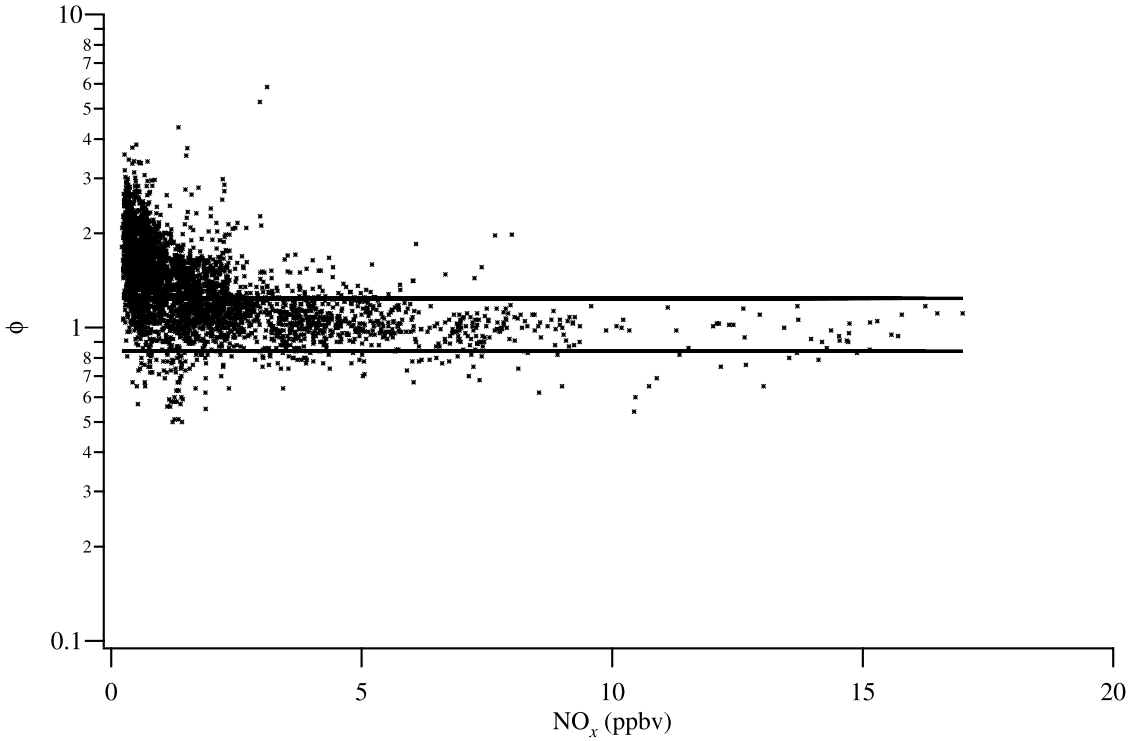

Figure 7. Calculated Φ values versus total measured NO_x (ppbv) over the course of the ICARTT campaign at TF. Solid lines indicate the range of Φ values that would be considered within photostationary state on the basis of measurement uncertainties.

values included in Figure 5, the average value of Φ is 1.38 ± 0.44 (SD). However, it is of greatest interest to explain the points in time with larger deviations from the photostationary state, as discussed below.

3.2. Meteorological Controls on Φ

[21] It must be determined whether the observed deviations from photostationary state are a result of physical or chemical phenomena. To that end, the Φ values calculated using equation (2) and exhibited in Figure 5 have been compared to wind speed, wind direction, temperature, relative humidity (RH), and j_{NO2}, which are all measured at TF with a resolution of 1 min.

[22] Regression analyses performed on a daily basis, as well as on the data set as a whole, indicated that values of the Leighton ratio are independent of wind speed and wind direction. For the entire data set, the R^2 values are 0.06 and 0.02, respectively, for wind speed and wind direction. This indicates that the strong deviation from Φ values equal to unity is likely a local phenomenon that does not depend on transport or transport speed from a specific upwind location. On a daily basis, the R^2 values ranged from 7.0E-05 to 0.53 for wind speed and from 1.0E-05 to 0.10 for wind direction. These findings are in contrast to calculations of Φ performed by *Mannschreck et al.* [2004] for data collected on the Hohenpeissenberg, where Φ was only significantly greater than 2.0 when the measured air mass had been transported from a specific wind direction.

[23] Correlations of Φ with temperature and RH are moderately stronger than those for wind speed and direction but are also weak. For the entire data set, the R^2 values are 0.13 and 0.20 for temperature and RH, respectively. The relationship with temperature is positive, and that with RH is negative. The daily ranges of R^2 are 0.01 to 0.53 for temperature and 4.0E-03 to 0.54 for RH. During daylight, temperature is generally higher, and RH is generally lower, explaining the positive and negative relationship each variable has with Φ because of its diurnal profile. There are examples during the ICARTT period when no relationship between temperature or RH and Φ exists. From investigation of the data, steep temporal gradients in temperature and RH are observable during certain days. This occurred without strong simultaneous shifts in solar radiation and without notable changes in calculated Φ values. Therefore the improved regressions with temperature and RH are more likely to be related to diurnal solar patterns.

[24] Of the meteorological variables considered for regression with Φ, the strongest relationship was found for j_{NO2}. For the entire data set, R^2 is 0.41, which still indicates a fairly weak relationship, despite being significantly larger than all other regression coefficients when applied to the entire data set. The range for individual days ranged from 0.03 to 0.68. The weakest relationship was observed on days of weakest sunlight. Because of these weak, but improved, regressions, it is hypothesized that strong solar radiation controls some chemical process(es) that then exert(s) an influence on Φ.

3.3. Chemical Controls on Φ

[25] Besides the species that potentially influence PO_2 or X levels, the other natural candidates to exert a chemical control on the Leighton ratio are the constituents of NO_x themselves. Figure 7 presents the inverse relationship between the calculated Φ values and the measured total

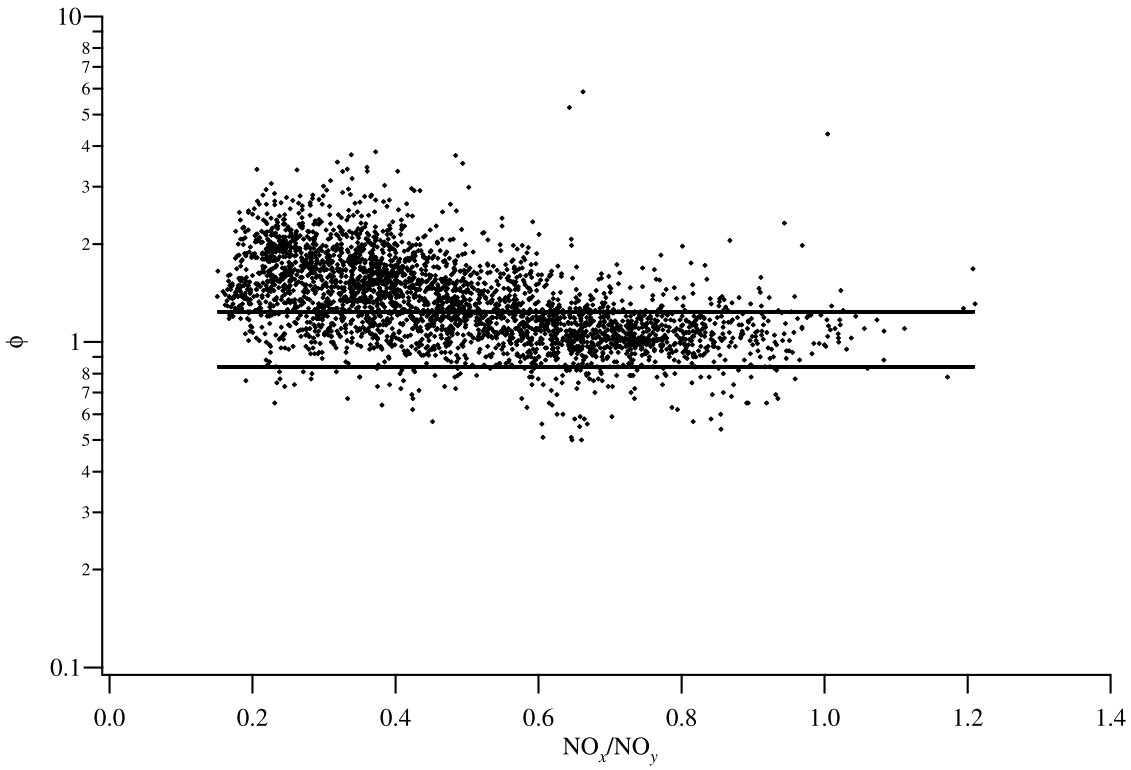

Figure 8. Calculated Φ values versus the ratio (dimensionless) of total measured NO_x to total measured NO_y over the course of the ICARTT campaign at TF. Solid lines indicate the range of Φ values that would be considered within photostationary state on the basis of measurement uncertainties.

NO_x. The range that is considered as adhering to photostationary state is indicated by the two solid lines. Larger mixing ratios of total NO_x clearly show adherence to photostationary state, while smaller values (generally less than 3 ppbv) tend to show deviations, which is consistent with NO_x dominating PO_2 loss at higher values of NO_x. It is of interest, therefore, to determine what other species may influence Φ values, particularly at times when total NO_x mixing ratios are less than 3 ppbv.

[26] In addition, the NO_x to NO_y ratio should be considered when investigating deviations from photochemical stationary state. Figure 8 indicates this relationship and shows that deviations of Φ from unity are more likely to occur when the NO_x to NO_y ratio is less than 0.5, indicating a more processed air mass. This relationship generally corresponds to Φ values that peak during the afternoon, as specified in Figure 5.

[27] As stated above, deviations from Leighton ratios of unity can generally be ascribed to the abundance of PO_2 or to halogen chemistry. Biogenic hydrocarbons and CO dominate OH reactivity at this location in summer [*Griffin et al.*, 2004a; M. White et al., Volatile organic compound measurements at Thompson Farm, NH, and Appledore Island, ME: A comparison of relative reactivities and variability, unpublished manuscript, 2007]. Therefore any deviation of Φ from photostationary state may be caused by PO_2 related to these species. An overall regression between CO and Φ yields no relationship, with an R^2 of 0.01 and a slightly negative slope (not shown). In addition, unlike NO_x, Φ values show no inclination for higher values at a specific threshold mixing ratio. On a daily basis, the R^2 value for this regression ranges from 4.0E-04 to 0.27. Despite this weak relationship, it cannot be concluded that HO_2 formed from the oxidation of CO by OH is negligible with respect to the significant deviation from photostationary state observed at TF because HO_2 variability is driven more by variability in OH than by variability in CO.

[28] A similar regression between isoprene (chosen as the predominant VOC based on reactivity) mixing ratios and Φ values is indicated in Figure 9a. Here, 10-min averaged Φ values are used, corresponding to the 10-min averaged mixing ratios of isoprene. Points are shaded by j_{NO2}. It is clear from Figure 9a that no strong linear relationship exists between measured isoprene mixing ratios and calculated Φ values. However, as with NO_x, a general increase in Φ can be observed at low mixing ratios of isoprene. Likewise, a scatterplot between the representative halogenated methane compound CH_2ClI and Φ (Figure 9b) shows similar behavior. The low mixing ratios of representative species that are either anthropogenic or biogenic, high j_{NO2} values, and low ratios of NO_x to NO_y that are all coincident with the high values of Φ support the hypothesis that Φ values depend inherently on strong photochemistry. This is despite the fact that emissions of isoprene are likely highest under conditions of strong sunlight. In addition, the hypothesis that photochemistry, not different emissions sources, controls Φ is supported by the lack of a relationship between Φ and wind characteristics.

3.4. Estimates of PO_2 Influence

[29] If it is assumed that PO_2 is the sole contributor to the observed deviations from photostationary state, an

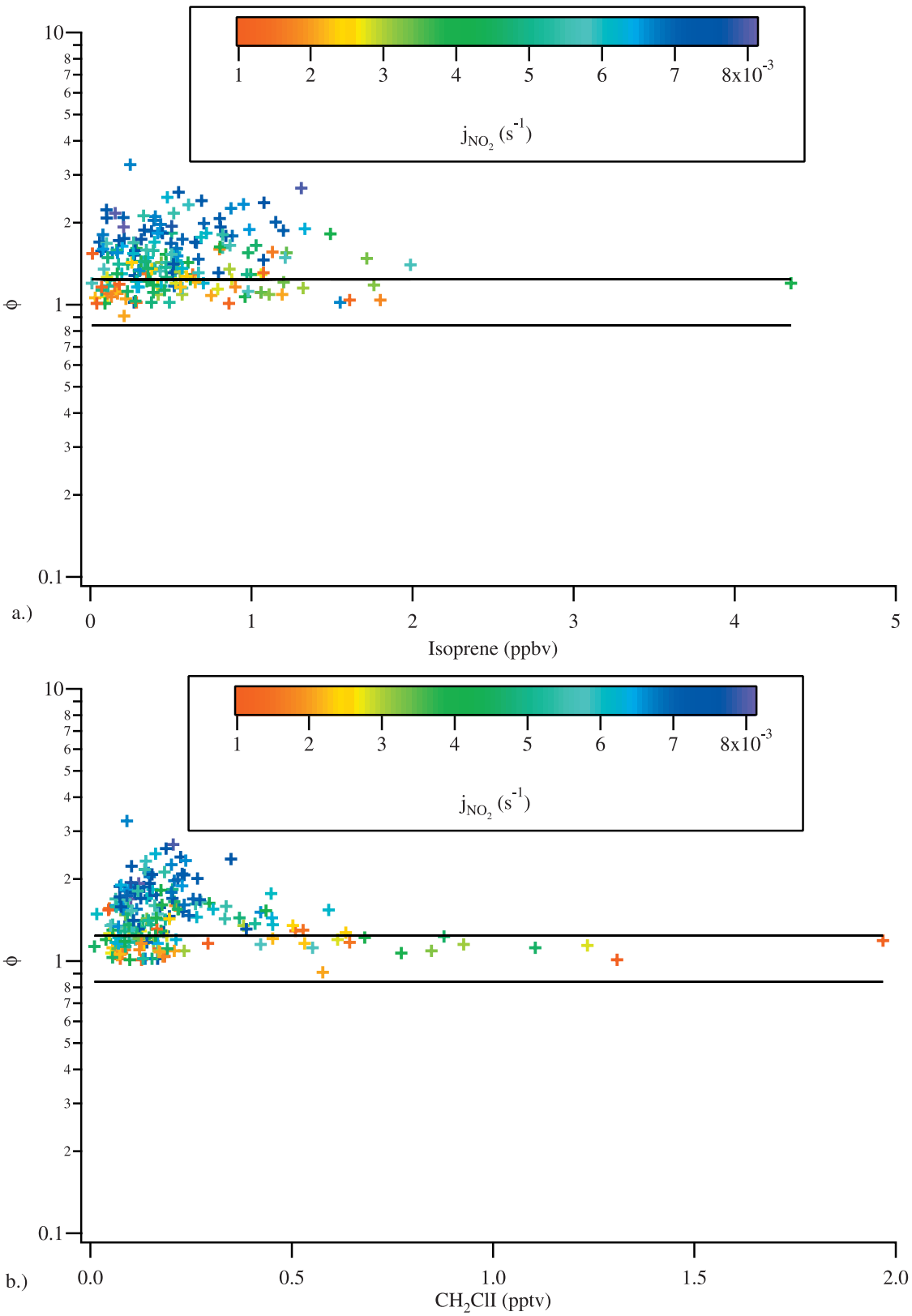

Figure 9. Calculated Φ values versus (a) isoprene and (b) CH_2ClI mixing ratios at TF over the course of the ICARTT campaign shaded by j_{NO2}. Considerably fewer data points are shown here because of the longer temporal resolution and less frequent measurements of organic gases compared to NO_x. Leighton ratio values have been averaged to the same timescale as the organic gas mixing ratio. Solid lines indicate the range of Φ values that would be considered within photostationary state on the basis of measurement uncertainties.

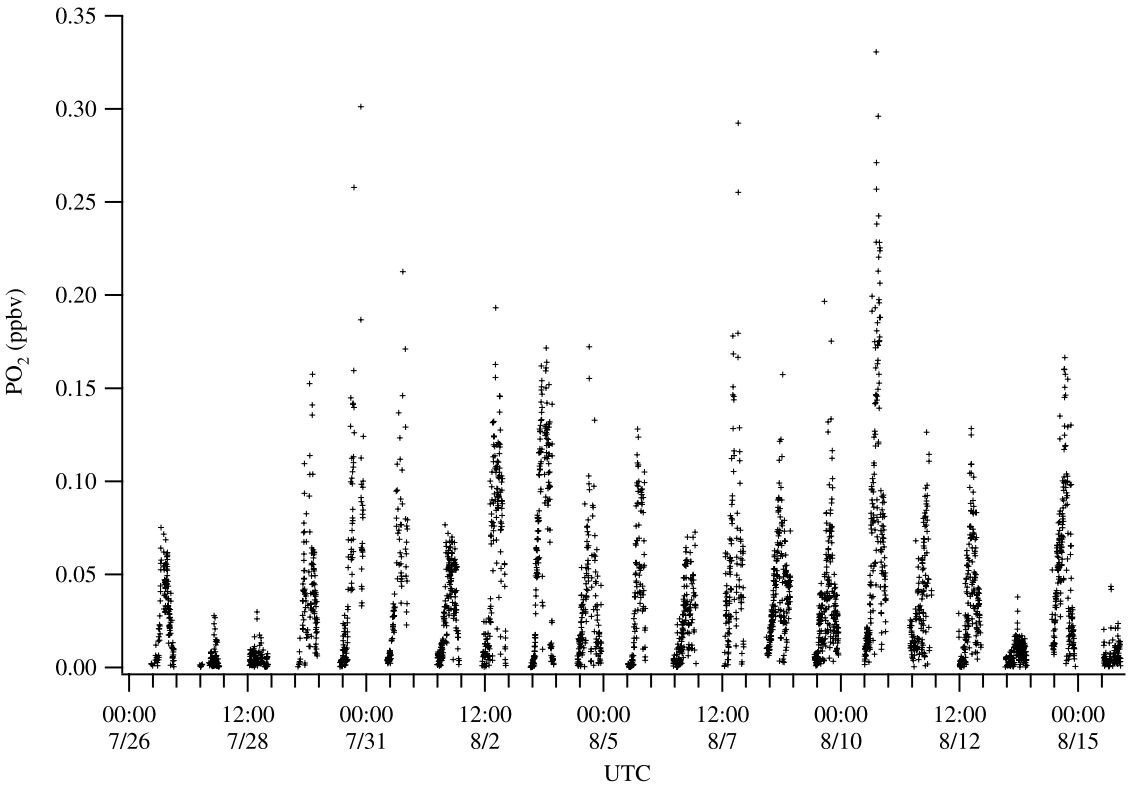

Figure 10. Mixing ratios of PO_2 (ppbv) that would force Φ values to be equal to 1.0 at TF at those times during the ICARTT campaign when $\Phi > 1.0$.

estimated PO_2 mixing ratio can be calculated by adding a second term (k_2[NO][PO_2]) to the denominator of equation (2), setting Φ equal to 1.0, and solving for [PO_2]:

$$[PO_2] = \frac{j_{NO_2}[NO_2]}{k_2[NO]} - \frac{k_1[O_3]}{k_2} \quad (4)$$

where k_2 is the temperature-dependent rate coefficient (ppbv^{-1} s^{-1}) for the reaction between HO_2 and NO. It is assumed that the rate coefficients for reactions between individual RO_2 molecules and NO are equivalent to this value [*DeMore et al.*, 1997]. In this scenario, it is the PO_2 reaction with NO that converts NO to NO_2 in excess of the NO and O_3 reaction. On the basis of equation (4), the required PO_2 level for those times when calculated Φ is greater than 1.0 ranges from approximately 1.1E-04 ppbv to 0.33 ppbv, with an average of 0.04 ± 0.04 (SD) ppbv for the entire data set. An average PO_2 mixing ratio between 0.02 and 0.03 ppbv was modeled for a similar time period during NEAQS (August 2002) at TF by *Griffin et al.* [2004a]; this value qualitatively agrees with the numbers indicated here. The time series of required PO_2 needed to bring Φ values equal to 1.0 is shown in Figure 10. Clearly, the temporal profile of PO_2 follows that of the Φ values presented in Figure 5.

[30] Numerous studies have measured PO_2 mixing ratios directly, used the method described here to quantify them, or applied radical budget or photochemical modeling techniques to estimate them. The variety of locations and seasons for which these measurements and calculations have been performed make a direct comparison difficult. However, a qualitative comparison is given here. Measurements of PO_2 using chemical amplification and other techniques have shown average mixing ratios on the order of tens of pptv in locations ranging from Hawaii to the Canary Islands to Mace Head to rural Germany [*Hauglustaine et al.*, 1996; *Zenker et al.*, 1998; *Carslaw et al.*, 1999; *Mihelcic et al.*, 2003]. During the ROSE campaign during summer 1990, *Cantrell et al.* [1993] measured PO_2 mixing ratios as high as approximately 300 pptv in rural Alabama. Radical budget and photochemical steady state models predict PO_2 mixing ratios that are generally on the same order of magnitude [*Kleinman et al.*, 1995; *Frost et al.*, 1998]. Calculations of PO_2 from expressions similar to equation (4) result in estimates of the PO_2 mixing ratio that are generally in accord with those presented here, despite differences in location and season [*Ridley et al.*, 1992; *Kleinman et al.*, 1995; *Carpenter et al.*, 1998; *Frost et al.*, 1998; *Rohrer et al.*, 1998; *Baumann et al.*, 2000; *Duderstadt et al.*, 1998; *Volz-Thomas et al.*, 2003; *Yang et al.*, 2004]. In general, PO_2 mixing ratios calculated by forcing Φ values to adhere to photostationary state are larger than those measured, indicating that there is likely another reaction occurring that converts NO to NO_2. The ratio of estimated to measured PO_2 on average is 1.23 for the work of *Cantrell et al.* [1993] and in the range of 2.0 to 3.0 for that of *Hauglustaine et al.* [1996] and *Mannschreck et al.* [2004]. PO_2 mixing ratios calculated using some form of equation (4) also tend to be larger than those calculated using radical budget calculations or modeling techniques [*Frost et al.*, 1998; *Volz-Thomas et al.*, 2003], with this discrepancy being as much as two orders of magnitude

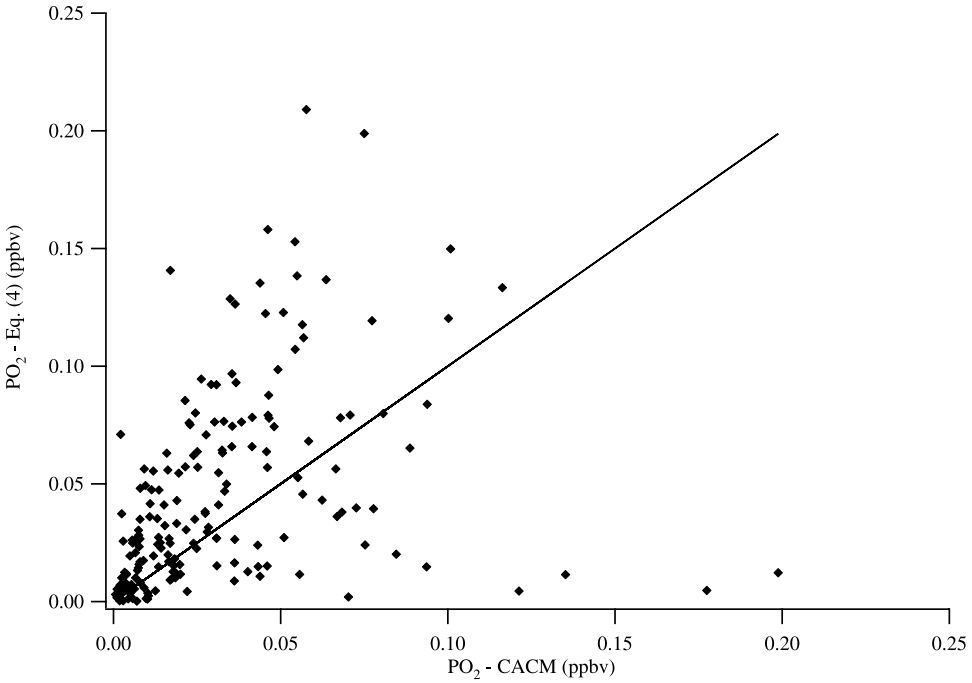

Figure 11. A comparison of mixing ratios of PO_2 predicted using equation (4) and predicted using CACM. The solid line represents a one-to-one relationship.

[*Carpenter et al.*, 1998]. However, adequate modeling results are achieved in some cases [*Ridley et al.*, 1992; *Kleinman et al.*, 1995].

[31] A zero-dimensional version of the Caltech Atmospheric Chemistry Mechanism (CACM) [*Griffin et al.*, 2002] is used with observed meteorological conditions and species mixing ratios to estimate HO_2 and total RO_2 mixing ratios over the 10-min periods of interest when VOC and NO_x measurements are temporally coincident. While the development of CACM was motivated by the desire to simulate SOA formation, particular attention was also paid to the chemistry of NO_x and VOCs containing fewer than six carbon atoms so that accurate O_3 prediction was also possible. CACM uses lumped (on the basis of structures and reaction rate constants) surrogates for VOCs and numerically solves kinetic rate expressions for over 120 different species. The pseudo steady state approximation is made for almost 70 individual organic radical species but is not made for HO_2 and the total RO_2 mixing ratio. The photolysis rates within CACM are scaled such that the j_{NO2} in the model is equivalent to that measured at TF. The performance and use of CACM has been documented previously [*Griffin et al.*, 2002, 2004b]. While CACM was developed for use in a highly polluted urban air basin [*Griffin et al.*, 2002], the chemistry occurring at TF is included in the mechanism because CACM considers the oxidation of C_1–C_{10} VOCs, including explicit treatment of isoprene. The version of CACM used incorporates all of the model improvements described by *Griffin et al.* [2005]. A comparison between PO_2 mixing ratios calculated using equation (4) for the relevant 10 min averages and PO_2 estimated using CACM is shown in Figure 11. With the exception of a few points in which CACM predicts significantly higher PO_2 mixing ratios than those determined using equation (4), it is observed that the majority of the points lie above the one-to-one line shown in Figure 11, as would be expected if species other than peroxy radicals were affecting the Leighton ratio values at this site.

[32] By including the reaction between NO and PO_2, a new Leighton ratio, termed here Φ_1, can be calculated as discussed previously:

$$\Phi_1 = \frac{j_{NO2}[NO_2]}{k_1[NO][O_3] + k_2[NO][PO_2]} \quad (5)$$

[33] To calculate Φ_1 using equation (5), measurements of NO, NO_2, and O_3 mixing ratios and j_{NO2} are used with calculated rate constants (based on measured temperatures) and estimated PO_2 mixing ratios (from CACM). Figure 12 indicates both Φ and Φ_1 values over the course of ICARTT to show how much of the deviation from unity can be attributed to PO_2 chemistry. On average, estimated PO_2 levels can account for approximately 71% of the observed departures of Φ from unity, which within uncertainty could be said to account for all of the deviation. It should also be noted that the PO_2 values calculated using CACM have uncertainties associated with heterogeneous HO_2 loss processes and halogen chemistry, as discussed by *Griffin* [2004].

3.5. Halogens

[34] It is assumed for the remainder of this discussion that the deviations of Φ_1 from unity in Figure 12 are due to the presence of halogens in the atmosphere at TF, as discussed by *Zhou et al.* [2005, also submitted manuscript, 2006]. In a manner similar to that used to derive equation (4), the product of the reaction rate constant of a halogen atom, k_{3X}, and the halogen atom concentration can be determined

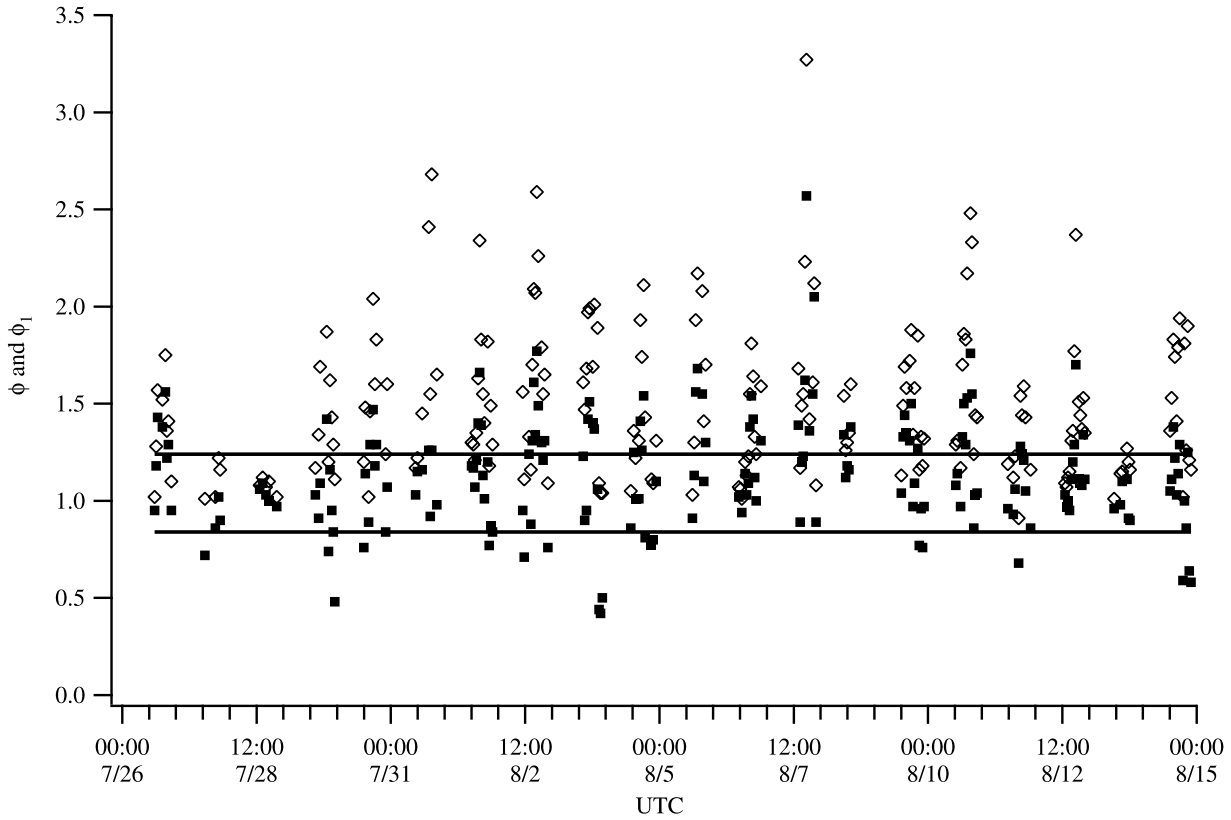

Figure 12. Comparison of Φ values (open diamonds) calculated using equation (2) and Φ_1 values (solid squares) calculated using equation (5) with $[PO_2]$ from CACM model output. Solid lines indicate the range of Φ values that would be considered within photostationary state on the basis of measurement uncertainties.

for those periods when Φ_1 is greater than 1.0, assuming that the halogen monoxide (XO) is in steady state:

$$k_{3X}[X] = \frac{j_{NO_2}[NO_2]}{[O_3]} - [NO]\left(k_1 + \frac{k_2[PO_2]}{[O_3]}\right) \quad (6)$$

[35] When combined with numerical values for k_{3X} for X = Cl or X = I [*DeMore et al.*, 1997; *Sander et al.*, 2006], it is possible to estimate the mixing ratios of Cl or I, assuming that they are the only halogen atom present. The possibility of X = Br is not considered here as the most photolabile halogenated methane compound observed at TF is CH_2ClI (Varner et al., manuscript in preparation, 2007). The application of equation (6) in this analysis forces only one type of halogen to be present at a time.

[36] Figure 13 indicates the Cl and I mixing ratios that would force Φ_1 to be 1.0, as calculated through equation (6). As would be expected, the temporal profiles of these halogen atoms follow those of Φ and Φ_1. Necessary Cl mixing ratios range from 0 to 0.6 pptv and have an average value of 0.07 pptv. The required I mixing ratios reach up to 1.2 pptv and have an average value of 0.14 pptv. On the basis of the relative strengths of the carbon-Cl and carbon-I bonds (Varner et al., manuscript in preparation, 2007), it is more likely that I is the halogen atom that is responsible for deviations of Φ from unity if it is assumed that CH_2ClI is the primary source of the halogen atoms. It should be noted that it is likely that Cl and I are each present and working in concert to lead to deviations of Φ from unity; however, a method that would allow an estimation of the combined effect of multiple halogens is not possible given the species currently measured at TF.

[37] It is possible to estimate the associated ClO and IO mixing ratios using a temperature-dependent rate constant for the reactions between XO and measured NO [*DeMore et al.*, 1997; *Sander et al.*, 2006]. The corresponding average ClO mixing ratio was 3.9 pptv (range up to 27 pptv). *Chang et al.* [2004] modeled summer Cl and ClO mixing ratios in the coastal marine boundary layer of Taiwan, with average respective values being approximately 0.01 pptv and 2.0 pptv. These estimates are on the same order of magnitude for those calculated for TF. The corresponding average IO mixing ratio was 8.7 pptv, with a maximum value of 64 pptv. *Peters et al.* [2005] observed average levels of IO up to 7.7 pptv during daylight hours in coastal European locations. While the IO levels calculated here are somewhat larger than those measured at Appledore Island during ICARTT (Varner et al., manuscript in preparation, 2007), the halogen levels estimated for TF appear to be atmospherically realistic given the level of qualitative agreement with values measured and modeled for other locations.

4. Conclusions

[38] Measurements of NO_x, O_3, and meteorological parameters made in semirural southeastern New Hampshire

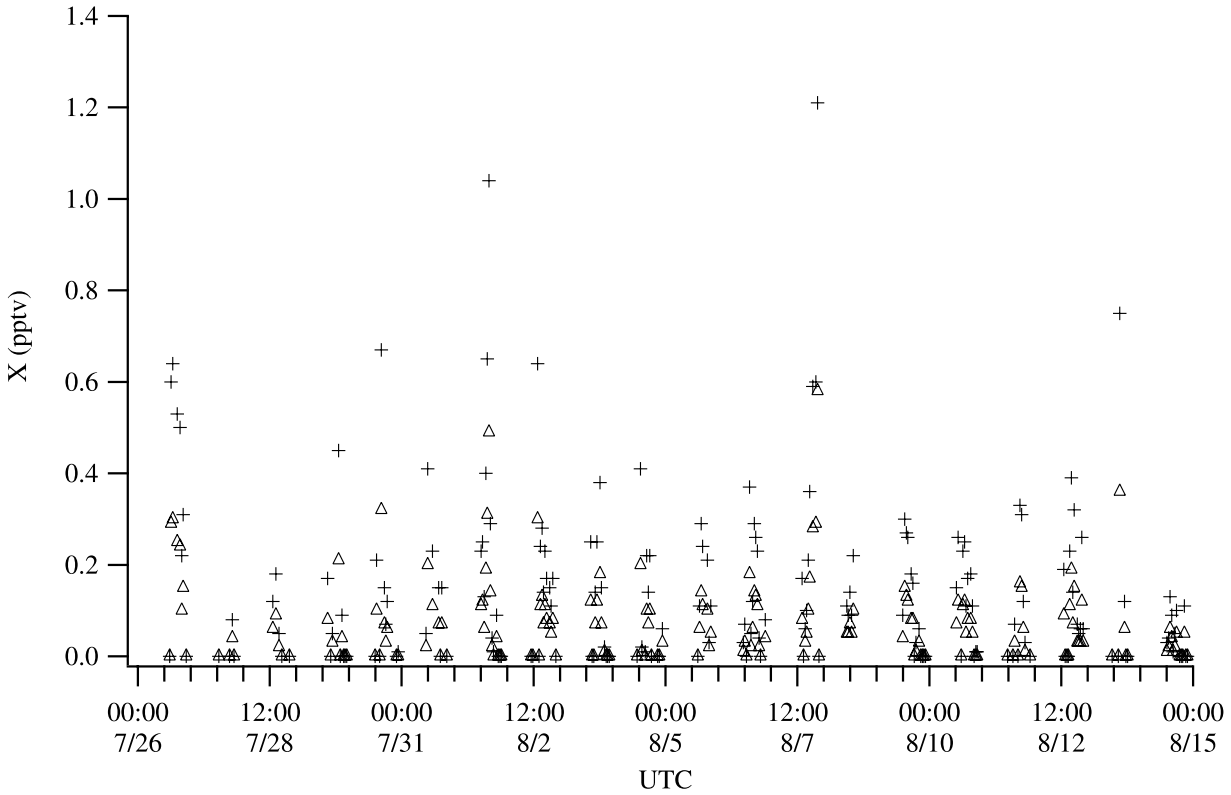

Figure 13. Chlorine (open triangles) and iodine (pluses) mixing ratios calculated using equation (6).

during the ICARTT campaign indicate significant deviations from traditional photostationary state, according to calculations of the Leighton ratio, Φ. These deviations occur under conditions of low NO_x mixing ratios, low NO_x to NO_y ratios, and when precursors to PO_2 and X appear to have been consumed photochemically. Such photochemical consumption is favored under strong sunlight conditions. A zero-dimensional photochemical model constrained by measurements estimates PO_2 levels significant enough to account for 71%, on average, of the observed positive deviations of $\Phi \geq 1.0$. The remainder of the deviations is assumed to result from X chemistry (at mixing ratios less than 1 pptv, most likely I) that is preceded by photolysis of photolabile halogenated methane compounds such as CH_2ClI.

[39] **Acknowledgments.** Financial support for this work was provided in part by the Office of Oceanic and Atmospheric Research of NOAA under AIRMAP grants NA03OAR4600122 and NA04OAR4600154 and in part by the National Science Foundation through grant ATM0327643. Any opinions, findings, conclusions and/or recommendations expressed in this material are those of the authors and do not necessarily reflect the views of the funding agencies. The authors would also like to thank Greg Huey, Karen Garrison, and Andrea Crosby for assistance in the installation and operation of the NO_x instrument and the AIRMAP project team for continued operation and maintenance of the UNH Atmospheric Observatories.

References

Baumann, K., E. J. Williams, W. M. Angevine, J. M. Roberts, R. B. Norton, G. J. Frost, F. C. Fehsenfeld, S. R. Springston, S. B. Bertman, and B. Hartsell (2000), Ozone production and transport near Nashville, Tennessee: Results from the 1994 study at New Hendersonville, *J. Geophys. Res.*, *105*, 9137–9153.

Brown, S. S., et al. (2004), Night-time removal of NO_x in the summer marine boundary layer, *Geophys. Res. Lett.*, *31*, L07108, doi:10.1029/2004GL019412.

Calvert, J. G., and W. R. Stockwell (1983), Deviations from the O_3-NO-NO_2 photostationary state in tropospheric chemistry, *Can. J. Chem.*, *61*, 983–992.

Cantrell, C. A., et al. (1993), Peroxy radicals as measured in ROSE and estimated from photostationary state deviations, *J. Geophys. Res.*, *98*, 18,355–18,366.

Carpenter, L. J., K. C. Klemitshaw, R. A. Burgess, S. A. Penkett, J. N. Cape, and G. G. McFadyen (1998), Investigation and evaluation of the NO_x/O_3 photochemical state, *Atmos. Environ.*, *32*, 3353–3365.

Carslaw, N., D. J. Creasey, D. E. Heard, A. C. Lewis, J. B. McQuaid, M. J. Pilling, P. S. Monks, B. J. Bandy, and S. A. Penkett (1999), Modeling OH, HO_2, and RO_2 radicals in the marine boundary layer: 1. Model construction and comparison with field measurements, *J. Geophys. Res.*, *104*, 30,241–30,255.

Chang, C. T., T. H. Liu, and F. T. Jeng (2004), Atmospheric concentrations of the Cl atom, ClO radical, and HO radical in the coastal marine boundary layer, *Environ. Res.*, *94*, 67–74.

Chang, S. Y., E. McDonald-Buller, Y. Kimura, G. Yarwood, J. Neece, M. Russell, P. Tanaka, and D. Allen (2002), Sensitivity of urban ozone formation to chlorine emission estimates, *Atmos. Environ.*, *36*, 4991–5003.

Chin, M., D. J. Jacob, J. W. Munger, D. D. Parrish, and B. G. Doddridge (1994), Relationship of ozone and carbon monoxide over North America, *J. Geophys. Res.*, *99*, 14,565–14,573.

Crawford, J., et al. (1996), Photostationary state analysis of the NO_2-NO system based on airborne observations from the western and central North Pacific, *J. Geophys. Res.*, *101*, 2053–2072.

Davis, D. D., et al. (1993), A photostationary state analysis of the NO_2-NO system based on airborne measurements from the subtropical/tropical north and south Atlantic, *J. Geophys. Res.*, *98*, 23,501–23,523.

DeBell, L. J., M. Vozella, R. W. Talbot, and J. E. Dibb (2004), Asian dust storm events of spring 2001 and associated pollutants observed in New England by the Atmospheric Investigation, Regional Modeling, Analysis and Prediction (AIRMAP) monitoring network, *J. Geophys. Res.*, *109*, D01304, doi:10.1029/2003JD003733.

DeMore, W. B., S. P. Sander, D. M. Golden, R. F. Hampson, M. J. Kurylo, C. J. Howard, A. R. Ravishankara, C. E. Kolb, and M. J. Molina (1997), Chemical kinetics and photochemical data for use in stratospheric modeling: Evaluation number 12, *JPL Publ., 97-4*, NASA Jet Propul. Lab., Pasadena, Calif.

Dibb, J. E., E. Scheuer, S. I. Whitlow, M. Vozella, E. Williams, and B. M. Lerner (2004), Ship-based nitric acid measurements in the Gulf of Maine during New England Air Quality Study 2002, *J. Geophys. Res.*, *109*, D20303, doi:10.1029/2004JD004843.

Duderstadt, K. A., et al. (1998), Photochemical production and loss rates of ozone at Sable Island, Nova Scotia during the North Atlantic Regional Experiment (NARE) 1993 summer intensive, *J. Geophys. Res.*, *103*, 13,531–13,555.

Fehsenfeld, F. C., et al. (2006), International Consortium for Atmospheric Research on Transport and Transformation (ICARTT): North America to Europe—Overview of the 2004 summer field study, *J. Geophys. Res.*, *111*, D23S01, doi:10.1029/2006JD007829.

Finlayson-Pitts, B. J., and J. N. Pitts Jr. (2000), *Chemistry of the Upper and Lower Atmosphere*, Elsevier, New York.

Fishman, J., and W. Seiler (1983), Correlative nature of ozone and carbon monoxide in the troposphere: Implications for the tropospheric ozone budget, *J. Geophys. Res.*, *88*, 3662–3670.

Frost, G. J., et. al. (1998), Photochemical ozone production in the rural southeastern United States during the 1990 Rural Oxidants in the Southern Environment (ROSE) program, *J. Geophys. Res.*, *103*, 22,491–22,508.

Gao, S., M. Keywood, N. L. Ng, J. Surratt, V. Varutbangkul, R. Bahreini, R. C. Flagan, and J. H. Seinfeld (2004), Low-molecular weight and oligomeric components in secondary organic aerosol from the ozonolysis of cycloalkenes and alpha-pinene, *J. Phys. Chem. A*, *108*, 10,147–10,164.

Glassman, I. (1996), *Combustion*, Elsevier, New York.

Griffin, R. J. (2004), Modeling the oxidative capacity of the atmosphere of the South Coast Air Basin of California: 2. HO_x radical production, *Environ. Sci. Technol.*, *38*, 753–757.

Griffin, R. J., D. R. Cocker III, R. C. Flagan, and J. H. Seinfeld (1999), Organic aerosol formation from the oxidation of biogenic hydrocarbons, *J. Geophys. Res.*, *104*, 3555–3567.

Griffin, R. J., D. Dabdub, and J. H. Seinfeld (2002), Secondary organic aerosol 1. Atmospheric chemical mechanism for production of molecular constituents, *J. Geophys. Res.*, *107*(D17), 4332, doi:10.1029/2001JD000541.

Griffin, R. J., C. A. Johnson, R. W. Talbot, H. Mao, R. S. Russo, Y. Zhou, and B. C. Sive (2004a), Quantification of ozone formation metrics at Thompson Farm during the New England Air Quality Study (NEAQS) 2002, *J. Geophys. Res.*, *109*, D24302, doi:10.1029/2004JD005344.

Griffin, R. J., M. K. Revelle, and D. Dabdub (2004b), Modeling the oxidative capacity of the atmosphere of the South Coast Air Basin of California. 1. Ozone formation metrics, *Environ. Sci. Technol.*, *38*, 746–752.

Griffin, R. J., D. Dabdub, and J. H. Seinfeld (2005), Development and initial evaluation of a dynamic species-resolved model for gas-phase chemistry and size-resolved gas/particle partitioning associated with secondary organic aerosol formation, *J. Geophys. Res.*, *110*, D05304, doi:10.1029/2004JD005219.

Hari, P., M. Raivonen, T. Vesala, J. W. Munger, K. Pilegaard, and M. Kulmala (2003), Atmospheric science—Ultraviolet light and leaf emission of NO_x, *Nature*, *422*, 134.

Hauglustaine, D. A., S. Madronich, B. A. Ridley, J. G. Walega, C. A. Cantrell, R. E. Shetter, and G. Hübler (1996), Observed and model-calculated photostationary state at Mauna Loa Observatory during MLOPEX2, *J. Geophys. Res.*, *101*, 14,681–14,696.

Hoffmann, T., J. R. Odum, F. Bowman, D. Collins, D. Klockow, R. C. Flagan, and J. H. Seinfeld (1997), Formation of organic aerosols from the oxidation of biogenic hydrocarbons, *J. Atmos. Chem.*, *26*, 189–222.

Kleinman, L. I., Y.-N. Lee, S. R. Springston, J. H. Lee, L. Nunnermacker, J. Weinstein-Lloyd, X. Zhou, and L. Newman (1995), Peroxy radical concentration and ozone formation rate at a rural site in the southeastern United States, *J. Geophys. Res.*, *100*, 7263–7273.

Knipping, E. M., M. J. Lakin, K. L. Foster, P. Jungwirth, D. J. Tobias, B. D. Gerber, D. Dabdub, and B. J. Finlayson-Pitts (2000), Experiments and simulations of ion-enhanced interfacial chemistry on aqueous NaCl aerosols, *Science*, *288*, 301–306.

Lefer, B. L., S. R. Hall, L. Cinquini, R. E. Shetter, J. D. Barrick, and J. H. Crawford (2001), Comparison of airborne NO_2 photolysis frequency measurements during PEM-Tropics B, *J. Geophys. Res.*, *106*, 32,645–32,656.

Leighton, P. A. (1961), *Photochemistry of Air Pollution*, Elsevier, New York.

Ludwig, J., F. X. Meixner, B. Vogel, and J. Forstner (2001), Soil-air exchange of nitric oxide: An overview of processes, environmental factors, and modeling studies, *Biogeochemistry*, *52*, 225–257.

Mannschreck, K., S. Gilge, C. Plass-Duelmer, W. Fricke, and H. Berresheim (2004), Assessment of the applicability of NO-NO_2-O_3 photostationary state to long-term measurements at the Hohenpeissenberg GAW Station, Germany, *Atmos. Chem. Phys.*, *4*, 1265–1277.

Mao, H., and R. Talbot (2004), O_3 and CO in New England: Temporal variations and relationships, *J. Geophys. Res.*, *109*, D21304, doi:10.1029/2004JD004913.

Mihelcic, D., et al. (2003), Peroxy radicals during BERLIOZ at Pabstthum: Measurements, radical budgets and ozone production, *J. Geophys. Res.*, *108*(D4), 8254, doi:10.1029/2001JD001014.

Nunnermacker, L. J., et al. (1998), Characterization of the Nashville urban plume on July 3 and July 18, 1995, *J. Geophys. Res.*, *103*, 28,129–28,148.

Parrish, D. D., M. Trainer, E. J. Williams, D. W. Fahey, G. Hübler, C. S. Eubank, S. C. Liu, P. C. Murphy, D. L. Albritton, and F. C. Fehsenfeld (1986), Measurements of the NO_x-O_3 photostationary state at Niwot Ridge, Colorado, *J. Geophys. Res.*, *91*, 5361–5370.

Peters, C., S. Pechtl, J. Stutz, K. Hebestreit, G. Honniger, K. G. Heumann, A. Schwarz, J. Winterlik, and U. Platt (2005), Reactive and organic halogen species in three different European coastal environments, *Atmos. Chem. Phys.*, *5*, 3357–3375.

Rattigan, O. V., D. E. Shallcross, and R. A. Cox (1997), UV absorption cross-sections and atmospheric photolysis rates of CF_3I, CH_3I, C_2H_5I, and CH_2ICl, *J. Chem. Soc. Faraday Trans.*, *93*, 2839–2846.

Ridley, B. A., S. Madronich, R. B. Chatfield, J. G. Walega, R. E. Shetter, M. A. Carroll, and D. D. Montzka (1992), Measurements and model simulations of the photostationary state during the Mauna Loa Observatory Photochemical Experiment: Implications for radical concentrations and ozone production and loss rates, *J. Geophys. Res.*, *97*, 10,375–10,388.

Rohrer, F., D. Brüning, E. S. Grobler, M. Weber, D. H. Ehhalt, R. Neubert, W. Schüssler, and I. Levin (1998), Mixing ratios and photostationary state of NO and NO_2 observed during the POPCORN field campaign at a rural site in Germany, *J. Atmos. Chem.*, *31*, 119–137.

Ryerson, T. B., E. J. Williams, and F. C. Fehsenfeld (2000), An efficient photolysis system for fast-response NO_2 measurements, *J. Geophys. Res.*, *105*, 26,447–26,461.

Sander, S. P., et al. (2006) Chemical kinetics and photochemical data for use in atmospheric studies: Evaluation number 15, *JPL Publ., 06-2*, NASA Jet Propul. Lab., Pasadena, Calif.

Seinfeld, J. H. (2004), Air pollution: A half century of progress, *AIChE J.*, *50*, 1096–1108.

Seinfeld, J. H., and S. N. Pandis (1998), *Atmospheric Chemistry and Physics*, Wiley-Interscience, Hoboken, N. J.

Shetter, R. E., D. H. Stedman, and D. H. West (1983), The $NO/NO_2/O_3$ photostationary state in Claremont, CA, *J. Air Pollut. Control Assoc.*, *33*, 212–214.

Sillman, S. (1995), The use of NO_y, H_2O_2, and HNO_3 as indicators for ozone-NO_x-hydrocarbon sensitivity in urban locations, *J. Geophys. Res.*, *100*, 14,175–14,188.

Sive, B. C., Y. Zhou, D. Troop, Y. L. Wang, W. C. Little, O. W. Wingenter, R. S. Russo, R. K. Varner, and R. W. Talbot (2005), Development of a cryogen-free concentration system for measurements of volatile organic compounds, *Anal. Chem.*, *77*, 6989–6998.

Stedman, D. H., and J. O. Jackson (1975), The photostationary state in photochemical smog, *Intl. J. Chem. Kinet. Symp.*, 493–501.

Talbot, R., H. Mao, and B. Sive (2005), Diurnal characteristics of surface level O_3 and other important trace gases in New England, *J. Geophys. Res.*, *110*, D09307, doi:10.1029/2004JD005449.

Thornton, J. A., et al. (2002), Ozone production rates as a function of NO_x abundances and HO_x production rates in the Nashville urban plume, *J. Geophys. Res.*, *107*(D12), 4146, doi:10.1029/2001JD000932.

Trainer, M., et al. (1993), Correlation of ozone with NO_y in photochemically aged air, *J. Geophys. Res.*, *98*, 2917–2925.

Volz-Thomas, A., H. Pätz, N. Houben, S. Konrad, D. Mihelcic, T. Klüpfel, and D. Perner (2003), Inorganic trace gases and peroxy radicals during BERLIOZ at Pabstthum: An investigation of the photostationary state of NO_x and O_3, *J. Geophys. Res.*, *108*(D4), 8248, doi:10.1029/2001JD001255.

Yang, J., R. E. Honrath, M. C. Peterson, D. D. Parrish, and M. Warshawsky (2004), Photostationary state deviation–estimated peroxy radicals and their implications for HO_x and ozone photochemistry at a remote northern Atlantic coastal site, *J. Geophys. Res.*, *109*, D02312, doi:10.1029/2003JD003983.

Zenker, T., et al. (1998), Intercomparison of NO, NO_2, O_3, and RO_x measurements during the Oxidizing Capacity of Tropospheric Atmosphere (OCTA) campaign 1993 at Izaña, *J. Geophys. Res.*, *103*, 13,615–13,634.

Zhou, Y., R. K. Varner, R. S. Russo, O. W. Wingenter, K. B. Haase, R. W. Talbot, and B. C. Sive (2005), Coastal water source of short-lived halocarbons in New England, *J. Geophys. Res.*, *110*, D21302, doi:10.1029/2004JD005603.

P. J. Beckman, R. J. Griffin, B. C. Sive, R. W. Talbot, and R. K. Varner, Climate Change Research Center, Institute for the Study of Earth, Oceans, and Space, University of New Hampshire, Durham, NH 03824, USA. (rob.griffin@unh.edu)